

Optimal drug dosing control for intensive care unit sedation by using a hybrid deterministic–stochastic pharmacokinetic and pharmacodynamic model

Behnood Gholami^{1,2}, Wassim M. Haddad^{3,*}, James M. Bailey⁴ and Allen R. Tannenbaum^{5,6}

¹*Department of Neurosurgery, Brigham and Women's Hospital, Harvard Medical School, Boston, MA 02115, USA*

²*Broad Institute of MIT and Harvard, Cambridge, MA 02142, USA*

³*School of Aerospace Engineering, Georgia Institute of Technology, Atlanta, GA 30332, USA*

⁴*Department of Anesthesiology, Northeast Georgia Medical Center, Gainesville, GA 30503, USA*

⁵*Department of Electrical and Computer Engineering, Boston University, Boston, MA 02215, USA*

⁶*Department of Biomedical Engineering, Boston University, Boston, MA 02215, USA*

SUMMARY

In clinical intensive care unit practice, sedative/analgesic agents are titrated to achieve a specific level of sedation. The level of sedation is currently based on clinical scoring systems. Examples include the motor activity assessment scale, the Richmond agitation–sedation scale, and the modified Ramsay sedation scale. In general, the goal of the clinician is to find the drug dose that maintains the patient at a sedation score corresponding to a moderately sedated state. This is typically done empirically, administering a drug dose that usually is in the effective range for most patients, observing the patient's response, and then adjusting the dose accordingly. However, the response of patients to any drug dose is a reflection of the pharmacokinetic and pharmacodynamic properties of the drug and the specific patient. In this paper, we use pharmacokinetic and pharmacodynamic modeling to find an optimal drug dosing control policy to drive the patient to a desired modified Ramsay sedation scale score. Copyright © 2012 John Wiley & Sons, Ltd.

Received 13 April 2011; Revised 14 March 2012; Accepted 25 May 2012

KEY WORDS: pharmacokinetics; pharmacodynamics; intensive care unit sedation; optimal control

1. INTRODUCTION

The clinical management of critically ill patients requiring mechanical ventilation due to respiratory failure is complex. Mechanical ventilation is intrinsically uncomfortable to the patient because of both the introduction of an artificial airway that is the interface between the patient and the ventilator, and the lack of synchronization between the patient's own spontaneous efforts to breathe and the action of the ventilator to breath for the patient. This can lead to the patient 'fighting the ventilator', which is not only uncomfortable for the patient but can also have deleterious physiological effects. For this reason, patients often require administration of sedative and analgesic agents in intensive care units (ICUs).

In clinical ICU practice, sedative/analgesic agents are titrated to achieve a specific level of sedation. The level of sedation is currently based on clinical scoring systems. Examples include the motor activity assessment scale (MAAS) [1], the Richmond agitation–sedation scale (RASS) [2], and the modified Ramsay sedation scale (MRSS) [3]. Specifically, in the MRSS scoring system,

*Correspondence to: Wassim M. Haddad, School of Aerospace Engineering, Georgia Institute of Technology, Atlanta, GA, 30332-0150, USA.

†E-mail: wm.haddad@aerospace.gatech.edu

patients are given an integer score of 0–6 as follows: 0 = paralyzed, unable to evaluate; 1 = awake; 2 = lightly sedated; 3 = moderately sedated, follows simple commands; 4 = deeply sedated, responds to nonpainful stimuli; 5 = deeply sedated, responds only to painful stimuli; and 6 = deeply sedated, unresponsive to painful stimuli.

Useful features of a sedation scale include multidisciplinary development, ease of utilization and interpretation with well-defined discrete criteria for each level, adequate granularity for effective drug titration, assessment of agitation, demonstration of interrater reliability for relevant patient populations, and evidence of validity. A number of sedation scales have been developed for ICU use that meet these criteria and have been tested for interrater reliability in multiple patient populations. In this paper, we specifically consider the MRSS scoring system; however, the framework presented herein can be adopted to any other sedation scoring system. The selection of MRSS was largely based on its simplicity, clinical familiarity, and convenience. The RASS score has greater granularity, and our techniques could be readily extended to its use. Finally, we assume that the patient's sedation level can always be evaluated, that is, the patient's MRSS sedation score of 1–6 can be assessed.

The goal of the clinician is to find the drug dose that maintains the patient at a sedation score of 3. This is typically done empirically, administering a drug dose that usually is in the effective range for most patients, observing the patient's response, and then adjusting the dose accordingly. However, the response of patients to any drug dose is a reflection of the pharmacokinetic and pharmacodynamic properties of the drug and the specific patient. In this paper, we use pharmacokinetic and pharmacodynamic modeling to find an optimal drug dose, as a function of time, to drive the patient to an MRSS score of 3. This framework is developed for a general n -compartment mammillary pharmacokinetic model, and the methodology can be applied to any sedative agent.

Although pharmacokinetics of sedative and anesthetic drugs can be adequately modeled by nonnegative and compartmental dynamical systems [4], the pharmacodynamics of these drugs are not well understood, and drug effect predictions usually involve probabilities [5–7]. Specifically, when considering sedative agents, drug effect is closely related to patient sedation level. As discussed in [6, 7], the corresponding sedation level of the ICU patient is related to drug concentration in the effect-site compartment by using an empirical probabilistic model.

In this paper, we model the pharmacokinetics and pharmacodynamics of a general sedative agent by using a hybrid deterministic–stochastic model involving deterministic pharmacokinetics and stochastic pharmacodynamics. Then, using this hybrid model, we consider the sedative drug propofol and use nonnegative and compartmental modeling to model the drug pharmacokinetics (drug concentration as a function of time), and a stochastic process to represent the patient's sedation score and model the drug pharmacodynamics (drug effect as a function of concentration). The first-order distribution of the stochastic process is a function of the states of the compartmental dynamical system.

Next, we use the aforementioned hybrid deterministic–stochastic model to develop an open-loop optimal control policy for ICU sedation. Specifically, we first find the optimal effect-site drug concentration corresponding to a high probability for the desired sedation score (i.e., MRSS score of 3) and a low probability for all other sedation scores. Then, we use optimal control theory to drive the effect-site drug concentration to the optimal value found in the previous step while minimizing a given cost functional. The cost functional captures control effort constraints as well as probability constraints associated with different sedation scores. The proposed methodology is then applied to a three-compartment nonlinear mammillary model describing the disposition of propofol to find an optimal drug dosing control policy to drive the patient to a desired MRSS score.

2. NOTATION AND MATHEMATICAL PRELIMINARIES

In this section, we introduce notation, several definitions, and some key results concerning nonlinear nonnegative dynamical systems [4] that are necessary for developing the main results of this paper. Specifically, for $x \in \mathbb{R}^n$, we write $x \geq 0$ (resp., $x \gg 0$) to indicate that every component of x is nonnegative (resp., positive). In this case, we say that x is *nonnegative* or *positive*, respectively. Likewise, $A \in \mathbb{R}^{n \times m}$ is nonnegative or positive if every entry of A is nonnegative or positive, which

is written as $A \ggg 0$ or $A \gg 0$, respectively. In addition, $\overline{\mathbb{R}}_+^n$ and \mathbb{R}_+^n denote the nonnegative and positive orthants of \mathbb{R}^n , that is, if $x \in \mathbb{R}^n$, then $x \in \overline{\mathbb{R}}_+^n$ and $x \in \mathbb{R}_+^n$ are equivalent, respectively, to $x \ggg 0$ and $x \gg 0$. Finally, we write $(\cdot)^T$ to denote transpose, $\|\cdot\|$ for a vector norm in \mathbb{R}^n , \mathbb{Z} to denote the set of integers, $\text{dist}(x, \mathcal{M})$ to denote the distance of a point $x \in \mathbb{R}^n$ to the set $\mathcal{M} \subseteq \mathbb{R}^n$ in the norm $\|\cdot\|$ (i.e., $\text{dist}(x, \mathcal{M}) \triangleq \inf_{p \in \mathcal{M}} \|x - p\|$), and \mathbf{e} to denote the ones vector of order n , that is, $\mathbf{e} \triangleq [1, \dots, 1]^T$.

The following definition introduces the notion of a nonnegative (resp., positive) function.

Definition 2.1

Let $T > 0$. A real function $u : [0, T] \rightarrow \mathbb{R}^m$ is a nonnegative (resp., positive) function if $u(t) \ggg 0$ (resp., $u(t) \gg 0$) on the interval $[0, T]$.

The following definition introduces the notions of essentially nonnegative and compartmental vector fields [4].

Definition 2.2

Let $f = [f_1, \dots, f_n]^T : \mathcal{D} \subseteq \overline{\mathbb{R}}_+^n \rightarrow \mathbb{R}^n$. Then, f is *essentially nonnegative* if $f_i(x) \geq 0$, for all $i = 1, \dots, n$, and $x \in \overline{\mathbb{R}}_+^n$ such that $x_i = 0$, where x_i denotes the i th component of x . f is *compartmental* if f is essentially nonnegative and $\mathbf{e}^T f(x) \leq 0$, $x \in \overline{\mathbb{R}}_+^n$.

Proposition 2.1

If $f(x) = Ax$, where $A \in \mathbb{R}^{n \times n}$, $x \in \mathbb{R}^n$, then f is essentially nonnegative if and only if $A_{(i,j)} \geq 0$, $i, j = 1, \dots, n$, $i \neq j$, where $A_{(i,j)}$ denotes the (i, j) th entry of A . Alternatively, f is compartmental if and only if $A_{(i,j)} \geq 0$, $i, j = 1, \dots, n$, $i \neq j$, and $\sum_{i=1}^n A_{(i,j)} \leq 0$, $j = 1, \dots, n$.

Proof

The proof is a direct consequence of Definition 2.2. □

In this paper, we consider controlled nonlinear dynamical systems of the form

$$\dot{x}(t) = f(x(t)) + G(x(t))u(t), \quad x(0) = x_0, \quad t \geq 0, \quad (1)$$

where $x(t) \in \mathbb{R}^n$, $t \geq 0$, $u(t) \in \mathbb{R}^m$, $t \geq 0$, $f : \mathbb{R}^n \rightarrow \mathbb{R}^n$ is locally Lipschitz continuous and satisfies $f(0) = 0$, $G : \mathbb{R}^n \rightarrow \mathbb{R}^{n \times m}$ is continuous, and $u : [0, \infty) \rightarrow \mathbb{R}^m$ is piecewise continuous.

The following definition and proposition are needed for the main results of the paper.

Definition 2.3

The nonlinear dynamical system given by (1) is nonnegative if, for every $x(0) \in \overline{\mathbb{R}}_+^n$ and $u(t) \ggg 0$, $t \geq 0$, the solution $x(t)$, $t \geq 0$, to (1) is nonnegative.

Proposition 2.2 ([4])

The nonlinear dynamical system given by (1) is nonnegative if $f : \mathbb{R}^n \rightarrow \mathbb{R}^n$ is essentially nonnegative and $G(x) \ggg 0$, $x \in \overline{\mathbb{R}}_+^n$.

It follows from Proposition 2.2 that if $f(\cdot)$ is essentially nonnegative, then a nonnegative input signal $G(x(t))u(t)$, $t \geq 0$, is sufficient to guarantee the nonnegativity of the state of (1).

Finally, the following theorem and definition are needed for the main results of the paper.

Theorem 2.1 ([8])

Let $x \in \mathbb{R}^n$, $\mathcal{M} \subseteq \mathbb{R}^n$ be a closed set and $\|\cdot\|$ be a norm in \mathbb{R}^n . Then, there exists $a_x \in \mathcal{M}$ such that $\|x - a_x\| = \text{dist}(x, \mathcal{M})$. Furthermore, if \mathcal{M} is closed and convex, and $\|\cdot\| : \mathbb{R}^n \rightarrow \overline{\mathbb{R}}_+$ is strictly convex, then a_x is unique.

Definition 2.4

Let $x \in \mathbb{R}^n$, $\mathcal{M} \subseteq \mathbb{R}^n$ be a closed set and $\|\cdot\|$ be a norm in \mathbb{R}^n . The projection of x on \mathcal{M} is given by

$$\text{proj}_{\mathcal{M}}(x) \triangleq \{a \in \mathcal{M} : \|x - a\| = \text{dist}(x, \mathcal{M})\}, \quad (2)$$

where $\text{proj}_{\mathcal{M}} : \mathbb{R}^n \rightarrow \mathbb{P}(\mathcal{M})$ and $\mathbb{P}(\mathcal{M})$ denotes the power set of \mathcal{M} .

Note that it follows from Theorem 2.1 and Definition 2.4 that if $p \in \text{proj}_{\mathcal{M}}(x)$, then $p = \text{argmin}_{a \in \mathcal{M}} \|x - a\|$. Finally, we note that if for every $x \in \mathbb{R}^n$ there exists a unique $p \in \text{proj}_{\mathcal{M}}(x)$, then \mathcal{M} is closed and convex [8].

3. NONLINEAR COMPARTMENTAL MAMMILLARY SYSTEMS

Drug dosing can be made more precise by using *pharmacokinetic* and *pharmacodynamic* modeling [9]. Pharmacokinetics is the study of the concentration of drugs in tissue as a function of time and dose schedule, whereas pharmacodynamics is the study of the relationship between drug concentration and drug effect. By relating dose to resultant drug concentration (pharmacokinetics) and concentration to effect (pharmacodynamics), a model for drug dosing can be generated.

Pharmacokinetic compartmental models typically assume that the body is comprised of multiple compartments. Within each compartment, the drug concentration is assumed to be uniform because of perfect, instantaneous mixing. Transport to other compartments and elimination from the body occur by metabolic processes. For simplicity, the transport rate is often assumed to be proportional to drug concentration. Although the assumption of instantaneous mixing is an idealization, it has little effect on the accuracy of the model as long as we do not try to predict drug concentrations immediately after the initial drug dose.

In this section, we consider a nonlinear compartmental *mammillary* dynamical system to model the pharmacokinetics of a sedative drug. The nonlinear mammillary model is comprised of a central compartment from which there is outflow from the system and which exchanges material reversibly with one or more peripheral compartments. In an n -compartment mammillary model, the central compartment, which is the site for drug administration, is generally thought to be comprised of the *intravascular blood* volume (i.e., blood within arteries and veins) as well as *highly perfused* organs (i.e., organs with high ratios of blood flow to weight) such as the heart, brain, kidneys, and liver. The central compartment exchanges drug with the peripheral compartments comprised of muscle, fat, and other organs and tissues of the body, which are metabolically inert as far as drug is concerned (Figure 1).

The pharmacokinetic model of an n -compartment nonlinear mammillary model with a control input drug dose needed to achieve and maintain a target drug concentration is given by

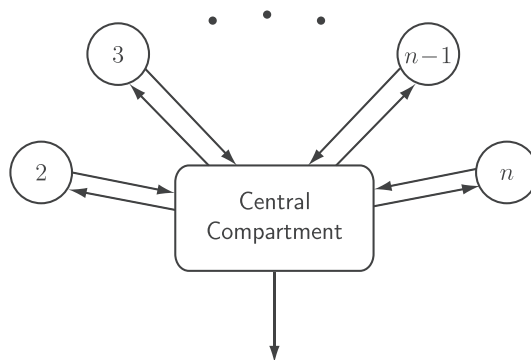


Figure 1. The n -compartment mammillary model.

$$\dot{x}_1(t) = - \left(\sum_{j=1}^n a_{j1}(c(t)) \right) x_1(t) + \sum_{j=2}^n a_{1j}(c(t)) x_j(t) + u(t), \quad x_1(0) = x_{10}, \quad t \geq 0, \quad (3)$$

$$\dot{x}_i(t) = a_{i1}(c(t)) x_1(t) - a_{1i}(c(t)) x_i(t), \quad x_i(0) = x_{i0}, \quad i = 2, \dots, n, \quad (4)$$

where $c(t) = x_1(t)/V_c$, V_c is the volume of the central compartment (about 15 l for a 70-kg patient), $a_{ij}(c)$, $i \neq j$ is the rate of transfer of drug from the j th to the i th compartment, $a_{11}(c)$ is the rate of drug metabolism and elimination (metabolism typically occurs in the liver), and $u(t)$, $t \geq 0$ is the infusion rate of the sedative drug into the central compartment.

Although the concentration of the sedative agent in the blood is correlated with lack of responsiveness [10], the concentration cannot be measured in real time. Because we are more interested in drug effect rather than drug concentration, we consider a model involving pharmacokinetics and pharmacodynamics for controlling consciousness. We use the sedation score to access the effect of anesthetic compounds on the brain. In Section 6, we utilize the modified probabilistic Hill equation [6] to model the relationship between the sedation score and the effect-site concentration. The effect-site compartment concentration is related to the concentration in the central compartment by the first-order model [11]

$$\dot{c}_{\text{eff}}(t) = a_{\text{eff}}(c(t) - c_{\text{eff}}(t)), \quad c_{\text{eff}}(0) = c(0), \quad t \geq 0, \quad (5)$$

where a_{eff} in min^{-1} is a positive time constant. In reality, the effect-site compartment equilibrates with the central compartment within a few minutes.

4. HYBRID PHARMACOKINETIC–PHARMACODYNAMIC MODEL AND OPTIMAL DRUG DOSING POLICY

In this section, we model the pharmacokinetics and pharmacodynamics of a sedative agent as a hybrid deterministic–stochastic model involving the deterministic pharmacokinetic model developed in Section 3, and a stochastic pharmacodynamic model. Next, we use this model to develop an open-loop optimal drug dosing control policy for ICU sedation.

To develop our optimal control policy for ICU sedation, we rewrite the pharmacokinetic system (3)–(5) as

$$\dot{x}(t) = f(x(t)) + Bu(t), \quad x(0) = x_0, \quad t \geq 0, \quad (6)$$

where $x = [x_1, \dots, x_n, c_{\text{eff}}]^T$, $B = [1, 0_{1 \times n}]^T$ and

$$f(x) \triangleq \begin{bmatrix} - \left(\sum_{j=1}^n a_{j1}(c) \right) x_1 + \sum_{j=2}^n a_{1j}(c) x_j \\ a_{21}(c) x_1 - a_{12}(c) x_2 \\ \vdots \\ a_{n1}(c) x_1 - a_{1n}(c) x_n \\ a_{\text{eff}}(c - c_{\text{eff}}) \end{bmatrix}. \quad (7)$$

Next, let the output $y(t)$ of the dynamical system (6) be given by a stochastic process. Specifically, for every $t \geq 0$, $y(t) = S(t)$ is a random variable with $\text{range}(S(t)) = \mathcal{S}$, where $\mathcal{S} \triangleq \{1, \dots, 6\}$. Let the first-order distribution of the stochastic process $S(t)$, $t \geq 0$, be given by $F_S(s, c_{\text{eff}}) = P(S(t) \leq s)$, where $s \in \mathbb{R}$, $F_S : \mathcal{S} \times \mathcal{C} \rightarrow \mathbb{R}$, and $\mathcal{C} \subset \overline{\mathbb{R}}_+$ is a set of feasible drug concentrations in the effect-site compartment. The first-order distribution $F_S(s, c_{\text{eff}})$ is identified using experiments and statistical techniques, and provides a probabilistic relationship between the effect-site drug concentration c_{eff} and the sedation score. Finally, define the mapping $F : \mathcal{C} \rightarrow \mathbb{R}^6$ by

$$F(c_{\text{eff}}) \triangleq [F_S(1, c_{\text{eff}}), \dots, F_S(6, c_{\text{eff}})]^T. \quad (8)$$

Our proposed approach for optimal drug dosing consists of two stages. In the first stage, the set of appropriate values of the drug concentration in the effect-site compartment denoted by C^* is identified such that the resulting probability distributions have desirable properties. More specifically, it is desirable to increase the probability associated with a desired sedation score (e.g., MRSS score of 3) and decrease the probabilities associated with all other levels of sedation. Ideally, we would like to target a cumulative distribution function for $S(t)$, $t > 0$, given by

$$F_{\text{step},S}(s) = \begin{cases} 0, & s < 3, \\ 1, & s \geq 3, \end{cases} \tag{9}$$

where $s \in \mathbb{R}$. Define $F_{\text{step}} \triangleq [0, 0, 1, 1, 1, 1]^T$ and note that, in general, $F_{\text{step}} \notin \mathcal{F}$, where $\mathcal{F} \triangleq F(\mathcal{C})$ is the image of $\mathcal{C} \subset \overline{\mathbb{R}}_+$ under $F : \mathcal{C} \rightarrow \mathbb{R}^6$ defining the set of feasible probability distributions given by

$$F(\mathcal{C}) \triangleq \{v : v = F(c) \text{ for some } c \in \mathcal{C}\}. \tag{10}$$

The following theorem and corollary provide a framework for identifying C^* given by

$$C^* \triangleq F^{-1}(\text{proj}_{\mathcal{F}}(F_{\text{step}})), \tag{11}$$

where $\mathcal{F} \triangleq F(\mathcal{C})$, $F^{-1}(\mathcal{B}) \triangleq \{c \in \mathcal{C} : F(c) \in \mathcal{B}\}$, $\mathcal{B} \subset \mathbb{R}^6$, and $\text{proj}_{\mathcal{F}}(F_{\text{step}})$ is the projection of F_{step} on \mathcal{F} .

Theorem 4.1

Assume that the set of feasible drug concentrations $\mathcal{C} \subset \overline{\mathbb{R}}_+$ is closed and the mapping $F : \mathcal{C} \rightarrow \mathbb{R}^6$ is continuous. Then, C^* given by (11) is not empty. Furthermore, if \mathcal{F} is convex, F is one-to-one, and $\|\cdot\| : \mathbb{R}^6 \rightarrow \overline{\mathbb{R}}_+$ is strictly convex, then C^* is a singleton.

Proof

Because \mathcal{C} is closed and F is continuous, \mathcal{F} is closed. Furthermore, it follows from Theorem 2.1 that there exists $G \in \mathcal{F}$ such that $\|F_{\text{step}} - G\| = \text{dist}(F_{\text{step}}, \mathcal{F})$, and hence, $G \in \text{proj}_{\mathcal{F}}(F_{\text{step}})$. Because $G \in \mathcal{F}$, there exists $c^* \in \mathcal{C}$ such that $F(c^*) = G$, and hence, $c^* \in C^*$, which proves that C^* is not empty. If \mathcal{F} is convex and $\|\cdot\| : \mathbb{R}^6 \rightarrow \overline{\mathbb{R}}_+$ is strictly convex, then it follows from Theorem 2.1 that $\text{proj}_{\mathcal{F}}(F_{\text{step}}) = \{G\}$. Now, because F is one-to-one, $C^* = \{c^*\}$. \square

Corollary 4.1

Assume that the set of feasible drug concentrations $\mathcal{C} \subset \overline{\mathbb{R}}_+$ is closed and the mapping $F : \mathcal{C} \rightarrow \mathbb{R}^6$ is continuous. Then,

$$F^{-1}(\text{proj}_{\mathcal{F}}(F_{\text{step}})) = \{c^* \in \mathcal{C} : c^* = \text{argmin}_{c \in \mathcal{C}} \|F_{\text{step}} - F(c)\|\}. \tag{12}$$

Proof

‘ \subseteq ’. Let $c^* \in F^{-1}(\text{proj}_{\mathcal{F}}(F_{\text{step}}))$. Then, it follows that $\|F_{\text{step}} - F(c^*)\| = \text{dist}(F_{\text{step}}, \mathcal{F})$, where $\mathcal{F} = F(\mathcal{C})$. Thus,

$$\begin{aligned} F(c^*) &= \text{argmin}_{F \in \mathcal{F}} \|F_{\text{step}} - F\| \\ &= \text{argmin}_{c \in \mathcal{C}} \|F_{\text{step}} - F(c)\|, \end{aligned} \tag{13}$$

and hence, $c^* \in \{c^* \in \mathcal{C} : c^* = \text{argmin}_{c \in \mathcal{C}} \|F_{\text{step}} - F(c)\|\}$, which proves ‘ \subseteq ’.

‘ \supseteq ’. Let $c^* = \text{argmin}_{c \in \mathcal{C}} \|F_{\text{step}} - F(c)\|$. Then, it follows that

$$\begin{aligned} \|F_{\text{step}} - F(c^*)\| &= \min_{c \in \mathcal{C}} \|F_{\text{step}} - F(c)\| \\ &= \min_{F \in \mathcal{F}} \|F_{\text{step}} - F\| \\ &= \text{dist}(F_{\text{step}}, \mathcal{F}), \end{aligned} \tag{14}$$

and hence, $c^* \in F^{-1}(\text{proj}_{\mathcal{F}}(F_{\text{step}}))$, which proves ‘ \supseteq ’. \square

Note that once \mathcal{C}^* is identified, an element of \mathcal{C}^* , denoted by c_{eff}^* , can be selected. The selected value $c_{\text{eff}}^* \in \mathcal{C}^*$ serves as the target drug concentration in the effect-site compartment. By using Corollary 4.1, c_{eff}^* can be identified by solving the optimization problem

$$\min_{c \in \mathcal{C}} \|F_{\text{step}} - F(c)\|. \quad (15)$$

Note that because it is desirable to reduce the probabilities associated with undersedation and oversedation, a specific norm can be used that enforces these properties. Specifically, we can choose the norm $\|\cdot\|_Q$, where $Q \in \mathbb{R}^{6 \times 6}$ is a positive-definite weighting matrix and $\|z\|_Q^2 \triangleq z^T Q z$, $z \in \mathbb{R}^6$. The weighting matrix Q can be used to assign weights (penalty) to different sedation levels. In particular, larger weighting values are assigned to sedation scores associated with undersedation and oversedation.

The second stage of the proposed optimal drug dosing policy involves an open-loop optimal control problem whose solution is given by the following theorem.

Theorem 4.2

Consider the pharmacokinetic model (6) with initial condition $x_0 = [x_{10}, \dots, x_{n0}, c_{\text{eff},0}]^T$. Let the optimal sedative drug infusion rate $u^*(t)$, $t \geq 0$, be given by the solution to the minimization problem

$$\min_{u(\cdot) \in \mathcal{U}} \int_0^T L(x(t), u(t)) dt, \quad (16)$$

subject to

$$g(x, u) \leq 0, \quad x \in \mathbb{R}^{n+1}, \quad u \in \mathbb{R}, \quad (17)$$

$$c_{\text{eff}}(T) = c_{\text{eff}}^*, \quad (18)$$

$$c_{\text{eff}}(t) \leq c_{\text{max}}, \quad (19)$$

where

$$L(x, u) \triangleq \|F(c_{\text{eff}}) - F(c_{\text{eff}}^*)\|_{R_1}^2 + \frac{1}{2} r_2 u^2, \quad (20)$$

$$g(x, u) \triangleq [g_1(x, u), g_2(u)]^T, \quad (21)$$

$$g_1(x, u) \triangleq (c_{\text{eff}} - c_{\text{max}})u, \quad (22)$$

$$g_2(u) \triangleq -u, \quad (23)$$

$c_{\text{eff}}^* \in \mathcal{C}^*$, \mathcal{C}^* is given by (11), $\mathcal{U} = \{u : [0, T] \rightarrow \mathbb{R} : u(\cdot) \text{ is piecewise continuous}\}$, $R_1 \in \mathbb{R}^{6 \times 6}$ is a given positive-definite matrix, and $r_2 > 0$ and $c_{\text{max}} > 0$ are given scalars. Then, $u^*(t)$, $t \geq 0$, is given by

$$u^*(t) = \frac{1}{r_2} [-\lambda_1(t) - (c_{\text{eff}} - c_{\text{max}})\mu(t) + \nu(t)], \quad (24)$$

where $\lambda_1(t)$, $\mu(t)$, and $\nu(t)$, $t \geq 0$, are the solutions to

$$\begin{aligned} \dot{\lambda}_1(t) = & \left\{ \left(\sum_{j=1}^n \frac{\partial a_{j1}(c)}{\partial c} \right) \frac{x_1(t)}{V_c} + \sum_{j=1}^n a_{j1}(c) - \sum_{j=2}^n \frac{\partial a_{1j}(c)}{\partial c} \frac{x_j(t)}{V_c} \right\} \lambda_1(t) \\ & - \sum_{j=2}^n \left(\frac{\partial a_{j1}(c)}{\partial c} \frac{x_1(t)}{V_c} + a_{j1}(c) - \frac{\partial a_{1j}(c)}{\partial c} \frac{x_j(t)}{V_c} \right) \lambda_j(t) - \frac{a_{\text{eff}}}{V_c} \lambda_{n+1}, \end{aligned} \quad (25)$$

$$\dot{\lambda}_i(t) = -a_{1i}(c)[\lambda_1(t) - \lambda_i(t)], \quad i = 2, \dots, n, \quad (26)$$

$$\begin{aligned} \dot{\lambda}_{n+1}(t) = & a_{\text{eff}}\lambda_{n+1}(t) - 2[F(c_{\text{eff}}(t)) - F(c_{\text{eff}}^*)]^T R_1 \frac{\partial F(c_{\text{eff}})}{\partial c_{\text{eff}}} \\ & - \mu(t) \frac{1}{r_2} [-\lambda_1(t) - (c_{\text{eff}} - c_{\text{max}})\mu(t) + v(t)], \end{aligned} \quad (27)$$

with boundary conditions

$$x(0) = x_0, \quad (28)$$

$$c_{\text{eff}}(T) = c_{\text{eff}}^*, \quad (29)$$

$$\lambda_i(T) = 0, \quad i = 1, \dots, n, \quad (30)$$

and $x(t), t \geq 0$, satisfying (6), $\mu(t) \geq 0, t \geq 0$, if $g_1(x(t), u(t)) = 0$, $\mu(t) = 0$ if $g_1(x(t), u(t)) < 0$, $v(t) \geq 0, t \geq 0$, if $g_2(u(t)) = 0$, and $v(t) = 0$ if $g_2(u(t)) < 0, t \geq 0$. Furthermore, $u^*(t) \geq 0, t \geq 0$, and $x(t) \geq 0, t \geq 0$, for all $x_0 \in \overline{\mathbb{R}}_+^{n+1}$.

Proof

Equations (24)–(27) are a direct consequence of the first-order necessary conditions for optimality of the optimization problem (16)–(19). Now, because $g(x, u) \leq 0, (x, u) \in \mathbb{R}^{n+1} \times \mathbb{R}$, it follows that $u^*(t) \geq 0, t \geq 0$. Finally, because $f(x)$ given by (7) is essentially nonnegative, it follows from Proposition 2.2 that $x(t) \geq 0, t \geq 0$, for all $x_0 \in \overline{\mathbb{R}}_+^{n+1}$. \square

Note that the cost functional given by (16) penalizes the control effort as well as the deviations from the cumulative distribution function $F(c_{\text{eff}}^*)$. In addition, the inequality constraints (17) and (19) ensure that the control input $u(t), t \geq 0$, is nonnegative and the drug concentration in the effect-site compartment does not exceed the maximum concentration c_{max} . Furthermore, the equality constraint (18) ensures that the drug concentration in the effect-site compartment reaches the target drug concentration c_{eff}^* in finite time T . Finally, the second-order Legendre–Clebsch necessary condition for optimality [12] is satisfied because $r_2 > 0$.

5. NONLINEAR PHARMACOKINETIC MODEL FOR DISPOSITION OF PROPOFOL

In this section, we use nonnegative and compartmental modeling to model the pharmacokinetics of the sedative agent propofol. Propofol, or 2,6-diisopropylphenol, is an intravenous hypnotic agent that, in low doses, can produce anxiolysis and, in higher doses, hypnosis (i.e., lack of responsiveness and consciousness). Propofol is widely used for ICU sedation because of this spectrum of pharmacodynamic effects and also its pharmacokinetics. It is typically administered as a continuous infusion and is a short-acting drug that can be readily titrated, that is, if the infusion rate is increased, then the blood level increases relatively quickly. Hence, the pharmacological effect of the drug can be quickly varied by varying the infusion rate.

Propofol is a *myocardial* depressant, that is, it decreases the contractility of the heart and lowers *cardiac output* (i.e., the volume of blood pumped by the heart per unit time). As a consequence, decreased cardiac output slows down redistribution kinetics, that is, the transfer of blood from the central compartment (heart, brain, kidneys, and liver) to the peripheral compartments (muscle and fat). In addition, decreased cardiac output could increase drug concentrations in the central compartment, causing even more myocardial depression and further decrease in cardiac output. This instability can lead to oversedation.

Oversedation increases risk to the patient because liberation from mechanical ventilation, one of the most common life-saving procedures performed in the ICU, may not be possible because of a diminished level of consciousness and respiratory depression from sedative drugs resulting in prolonged length of stay in the ICU. Prolonged ventilation is expensive and is associated with known

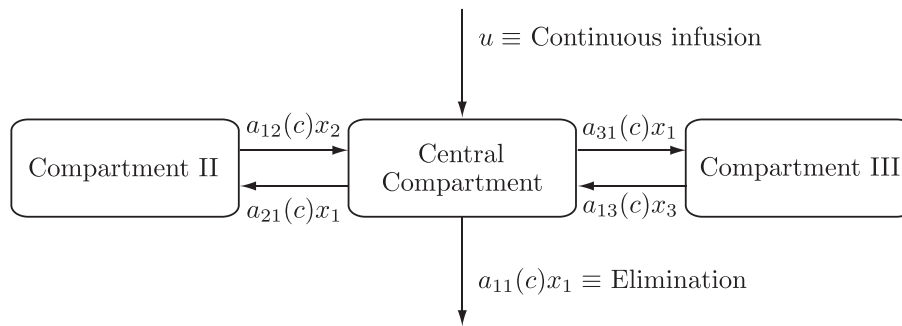


Figure 2. Pharmacokinetic model for disposition of propofol.

risks, such as inadvertent extubation, laryngotracheal trauma, and ventilator-associated pneumonia. Alternatively, undersedation leads to agitation and can result in dangerous situations for both the patient and the intensivist. Specifically, agitated patients can do physical harm to themselves by dislodging their endotracheal tube, which can potentially endanger their lives.

The pharmacokinetics of propofol are described by the three-compartment model [4, 13] shown in Figure 2, where x_1 denotes the mass of drug in the central compartment, which, as discussed in Section 3, is the site for drug administration and is generally thought to be comprised of the intravascular blood volume as well as highly perfused organs such as the heart, brain, kidneys, and liver. These organs receive a large fraction of the cardiac output. The remainder of the drug in the body is assumed to reside in two peripheral compartments, one identified with muscle and one with fat; the masses in these compartments are denoted by x_2 and x_3 , respectively. These compartments receive less than 20% of the cardiac output.

A mass balance of the three-state compartmental model yields

$$\dot{x}_1(t) = -[a_{11}(c(t)) + a_{21}(c(t)) + a_{31}(c(t))]x_1(t) + a_{12}(c(t))x_2(t) + a_{13}(c(t))x_3(t) + u(t),$$

$$x_1(0) = x_{10}, \quad t \geq 0, \quad (31)$$

$$\dot{x}_2(t) = a_{21}(c(t))x_1(t) - a_{12}(c(t))x_2(t), \quad x_2(0) = x_{20}, \quad (32)$$

$$\dot{x}_3(t) = a_{31}(c(t))x_1(t) - a_{13}(c(t))x_3(t), \quad x_3(0) = x_{30}, \quad (33)$$

where $c(t) = x_1(t)/V_c$, V_c is the volume of the central compartment (about 15 l for a 70-kg patient), $a_{ij}(c)$, $i \neq j$, is the rate of transfer of drug from the j th to the i th compartment, $a_{11}(c)$ is the rate of drug metabolism and elimination (metabolism typically occurs in the liver), and $u(t)$, $t \geq 0$, is the infusion rate of the sedative drug propofol into the central compartment. The transfer coefficients are assumed to be functions of the drug concentration c because it is well known that the pharmacokinetics of propofol are influenced by cardiac output [14] and, in turn, cardiac output is influenced by propofol plasma concentrations, both due to *venodilation* (pooling of blood in dilated veins) [15] and myocardial depression [16].

Experimental data indicate that the transfer coefficients $a_{ij}(\cdot)$ are nonincreasing functions of the propofol concentration [15, 16]. The most widely used empirical models for pharmacodynamic concentration–effect relationships are modifications of the Hill equation [17]. Applying this almost ubiquitous empirical model to the relationship between transfer coefficients implies that

$$a_{ij}(c) = A_{ij} Q_{ij}(c), \quad Q_{ij}(c) = \frac{Q_0 \tilde{C}_{50,ij}^{\alpha_{ij}}}{(\tilde{C}_{50,ij}^{\alpha_{ij}} + c^{\alpha_{ij}})}, \quad (34)$$

where, for $i, j \in \{1, 2, 3\}$, $i \neq j$, $\tilde{C}_{50,ij}$ is the drug concentration associated with a 50% decrease in the transfer coefficient, α_{ij} is a parameter that determines the steepness of the concentration–effect relationship, and A_{ij} are positive constants. Note that both pharmacokinetic parameters

are functions of i and j , that is, there are distinct Hill equations for each transfer coefficient. Furthermore, because for many drugs the rate of metabolism $a_{11}(c)$ is proportional to the rate of transport of drug to the liver, we assume that $a_{11}(c)$ is also proportional to the cardiac output so that $a_{11}(c) = A_{11}Q_{11}(c)$. Finally, the relationship between the effect-site and the central compartment is given by (5).

6. OPTIMAL DRUG DOSING POLICY FOR PROPOFOL

The framework presented in Section 4 is applicable to sedative agents for which a valid compartmental model capturing the pharmacokinetics and an associated probabilistic model capturing drug concentration and sedation score exist. In this section, we use the framework developed in Section 4 to model the pharmacokinetics and pharmacodynamics of propofol as a hybrid deterministic–stochastic model. Specifically, we use the deterministic pharmacokinetic model developed in Section 5. Next, we use this model to develop an open-loop optimal drug dosing control policy for ICU sedation.

In [6], the authors investigate the relationship between drug concentration and the ICU patient’s sedation score. Specifically, the sedation score is modeled as a random variable and an empirical cumulative distribution function, for this random variable is developed and validated for propofol-based sedation where the cumulative distribution function is a function of drug concentration at the effect site.

To develop our optimal control policy for ICU sedation, we rewrite the pharmacokinetic system (5), (31)–(33) as

$$\dot{x}(t) = f(x(t)) + Bu(t), \quad x(0) = x_0, \quad t \geq 0, \tag{35}$$

where $x = [x_1, x_2, x_3, c_{\text{eff}}]^T$, $B = [1, 0, 0, 0]^T$, and

$$f(x) \triangleq \begin{bmatrix} -(a_{11}(c) + a_{21}(c) + a_{31}(c))x_1 + a_{12}(c)x_2 + a_{13}(c)x_3 \\ a_{21}(c)x_1 - a_{12}(c)x_2 \\ a_{31}(c)x_1 - a_{13}(c)x_3 \\ a_{\text{eff}}(c - c_{\text{eff}}) \end{bmatrix}. \tag{36}$$

Next, let the output $y(t)$ of the dynamical system (35) be given by a stochastic process. Specifically, for every $t \geq 0$, $y(t) = S(t)$ is a random variable with $\text{range}(S(t)) = \mathcal{S}$, where $\mathcal{S} \triangleq \{1, \dots, 6\}$. The first-order distribution of the stochastic process $S(t)$ is given by [6],

$$F_S(s, c_{\text{eff}}) = P(S(t) \leq s) = \begin{cases} 0 & s < 1, \\ 1 - \frac{c_{\text{eff}}^\gamma(t)}{c_{\text{eff}}^\gamma(t) + C_{50,1,s}^\gamma + 1} & 1 \leq s < 6, \\ 1, & s \geq 6, \end{cases} \tag{37}$$

where $s \in \mathbb{R}$, $F_S : \mathcal{S} \times \mathcal{C} \rightarrow \mathbb{R}$ is a first-order distribution function of the stochastic process $S(t)$, $\mathcal{C} \subset \overline{\mathbb{R}}_+$ is a closed set of feasible drug concentrations in the effect-site compartment, $\lfloor \cdot \rfloor$ denotes the floor function defined by $\lfloor s \rfloor \triangleq \max_{z \in \mathbb{Z}} z \leq s$, and $\gamma > 0$ is a factor determining the steepness of the concentration–effect relationship. Finally, note that $F : \mathcal{C} \rightarrow \mathbb{R}^6$ given by (8) is continuous.

The second stage of the proposed optimal drug dosing policy involves an open-loop optimal control problem. Specifically, it follows from Theorem 4.2 that the optimal propofol infusion rate $u^*(t)$, $t \geq 0$, is given by the solution to the minimization problem (16) subject to (17)–(19), where $c_{\text{eff}}^* \in \mathcal{C}^*$, and \mathcal{C}^* is given by (11). In particular, $u^*(t)$, $t \geq 0$, is given by

$$u^*(t) = \frac{1}{r_2}[-\lambda_1(t) - (c_{\text{eff}} - c_{\text{max}})\mu(t) + v(t)], \tag{38}$$

where $\lambda_1(t)$, $\mu(t)$, and $\nu(t)$, $t \geq 0$, are the solutions to

$$\begin{aligned} \dot{\lambda}_1(t) = & \left[\left(\frac{\partial a_{11}(c)}{\partial c} + \frac{\partial a_{21}(c)}{\partial c} + \frac{\partial a_{31}(c)}{\partial c} \right) \frac{x_1(t)}{V_c} + a_{11}(c) + a_{21}(c) + a_{31}(c) \right. \\ & \left. - \frac{\partial a_{12}(c)}{\partial c} \frac{x_2(t)}{V_c} - \frac{\partial a_{13}(c)}{\partial c} \frac{x_3(t)}{V_c} \right] \lambda_1(t) \\ & + \left[-\frac{\partial a_{21}(c)}{\partial c} \frac{x_1(t)}{V_c} - a_{21}(c) + \frac{\partial a_{12}(c)}{\partial c} \frac{x_2(t)}{V_c} \right] \lambda_2(t) \\ & + \left[-\frac{\partial a_{31}(c)}{\partial c} \frac{x_1(t)}{V_c} - a_{31}(c) + \frac{\partial a_{13}(c)}{\partial c} \frac{x_3(t)}{V_c} \right] \lambda_3(t) - \frac{a_{\text{eff}}}{V_c} \lambda_4(t), \end{aligned} \quad (39)$$

$$\dot{\lambda}_2(t) = -a_{12}(c)\lambda_1(t) + a_{12}\lambda_2(t), \quad (40)$$

$$\dot{\lambda}_3(t) = -a_{13}(c)\lambda_1(t) + a_{13}(c)\lambda_3(t), \quad (41)$$

$$\begin{aligned} \dot{\lambda}_4(t) = & a_{\text{eff}}\lambda_4(t) - 2[F(c_{\text{eff}}(t)) - F(c_{\text{eff}}^*)]^T R_1 \frac{\partial F(c_{\text{eff}})}{\partial c_{\text{eff}}} \\ & - \mu(t) \frac{1}{r_2} [-\lambda_1(t) - (c_{\text{eff}} - c_{\text{max}})\mu(t) + \nu(t)], \end{aligned} \quad (42)$$

where

$$\begin{aligned} \frac{\partial a_{ij}(c)}{\partial c} = & \frac{-\alpha_{ij} c^{\alpha_{ij}-1} A_{ij} Q_0 \tilde{C}_{50,ij}^{\alpha_{ij}}}{(\tilde{C}_{50,ij}^{\alpha_{ij}} + c^{\alpha_{ij}})^2}, \quad i = 1, j = 1, \text{ and } i, j \in \{1, 2, 3\}, i \neq j, \\ \frac{\partial F(c_{\text{eff}})}{\partial c_{\text{eff}}} = & \left[-\frac{\gamma c_{\text{eff}}^{\gamma-1} C_{50,2}^{\gamma}}{(c_{\text{eff}}^{\gamma} + C_{50,2}^{\gamma})^2}, -\frac{\gamma c_{\text{eff}}^{\gamma-1} C_{50,3}^{\gamma}}{(c_{\text{eff}}^{\gamma} + C_{50,3}^{\gamma})^2}, -\frac{\gamma c_{\text{eff}}^{\gamma-1} C_{50,4}^{\gamma}}{(c_{\text{eff}}^{\gamma} + C_{50,4}^{\gamma})^2}, -\frac{\gamma c_{\text{eff}}^{\gamma-1} C_{50,5}^{\gamma}}{(c_{\text{eff}}^{\gamma} + C_{50,5}^{\gamma})^2}, -\frac{\gamma c_{\text{eff}}^{\gamma-1} C_{50,6}^{\gamma}}{(c_{\text{eff}}^{\gamma} + C_{50,6}^{\gamma})^2}, 0 \right]^T, \end{aligned}$$

with boundary conditions (28), (29), and $\lambda_1(T) = \lambda_2(T) = \lambda_3(T) = 0$, and $x(t)$, $t \geq 0$, satisfying (35), $\mu(t) \geq 0$, $t \geq 0$, if $g_1(x(t), u(t)) = 0$, $\mu(t) = 0$ if $g_1(x(t), u(t)) < 0$, $\nu(t) \geq 0$, $t \geq 0$, if $g_2(u(t)) = 0$, and $\nu(t) = 0$ if $g_2(u(t)) < 0$, $t \geq 0$. Furthermore, $u^*(t) \geq 0$, $t \geq 0$, and $x(t) \geq 0$, $t \geq 0$, for all $x_0 \in \mathbb{R}_+^4$.

Remark 6.1

The framework in this paper can be used for other sedative agents for which a valid compartmental model capturing the pharmacokinetics and an associated probabilistic model capturing drug concentration and sedation score exist. For example, the pharmacokinetics of *midazolam* (an alternative intravenous sedative agent used as a hypnotic) is described by a two-compartment model [18]. The empirical relationship between drug concentration and sedation score for midazolam is developed in [7]. By using an identical procedure as outlined previously, the optimal drug dosing policy for the midazolam infusion rate can be found.

7. ILLUSTRATIVE NUMERICAL EXAMPLE

In this section, we present a numerical example to demonstrate the efficacy of the proposed framework. For simplicity of exposition and to provide a nonlinear model to illustrate implementation of our open-loop optimal controller, we assume that \tilde{C}_{50} and α in (34) are independent of i and j [4]. Furthermore, because decreases in cardiac output are observed at clinically utilized propofol concentrations, we arbitrarily assign \tilde{C}_{50} a value of 4 $\mu\text{g/ml}$ because this value is in the mid-range of clinically utilized values. We also arbitrarily assign α a value of 3 [19]. This value is within the typical range of those observed for ligand–receptor binding [20]. Note that these assumptions

on \tilde{C}_{50} and α (both the independence from i and j and the assumed values) are done to provide a numerical framework for simulation. Even if these assumptions are incorrect, the basic Hill equations relating the transfer coefficients to propofol concentration are consistent with standard pharmacodynamic modeling.

For our simulation, we assume $V_c = (0.228 \text{ l/kg})(M \text{ kg})$, where $M = 70 \text{ kg}$ is the mass of the patient, $A_{21}Q_0 = 0.112 \text{ min}^{-1}$, $A_{12}Q_0 = 0.055 \text{ min}^{-1}$, $A_{31}Q_0 = 0.0419 \text{ min}^{-1}$, $A_{13}Q_0 = 0.0033 \text{ min}^{-1}$, $A_{11}Q_0 = 0.119 \text{ min}^{-1}$, $\alpha = 3$, and $\tilde{C}_{50} = 4 \mu\text{g/ml}$ [13, 19]. Note that the parameter values for α and \tilde{C}_{50} probably exaggerate the effect of propofol on cardiac output. They have been selected to accentuate nonlinearity, but they are not biologically unrealistic. Furthermore, in (37), we assume $C_{50,2} = 0.13 \mu\text{g/ml}$, $C_{50,3} = 0.50 \mu\text{g/ml}$, $C_{50,4} = 0.74 \mu\text{g/ml}$, $C_{50,5} = 1.48 \mu\text{g/ml}$, $C_{50,6} = 2.34 \mu\text{g/ml}$, and $\gamma = 1.7$ [6]. In addition, we assume $T = 5 \text{ min}$, $Q = R_1 = \text{diag}[17, 2, 1, 2, 17, 82]$, and $r_2 = 0.01$. By using (15), the optimal effect-site drug concentration was found to be $c_{\text{eff}}^* = 0.60294 \mu\text{g/ml}$.

For our simulation, we choose the diagonal matrix R_1 with diagonal entries given by $R_{1(i,i)} = (i - 3)^4 + 1$, $i = 1, \dots, 6$. This ensures that a larger weight (penalty) is assigned to sedation scores associated with undersedation and oversedation. The drug concentration of the central and the effect-site compartments as well as control input as a function of time are shown in Figures 3 and 4, respectively. The probability mass function of the sedation score is given in Figure 5 for $t = 0, 1, 3$, and 5 min . Note that at $t = 5 \text{ min}$, the probability that the patient has an MRSS sedation score of 2, 3, or 4 (i.e., the patient is lightly sedated, moderately sedated and follows simple commands, or deeply sedated and responds to nonpainful stimuli) is 75%.

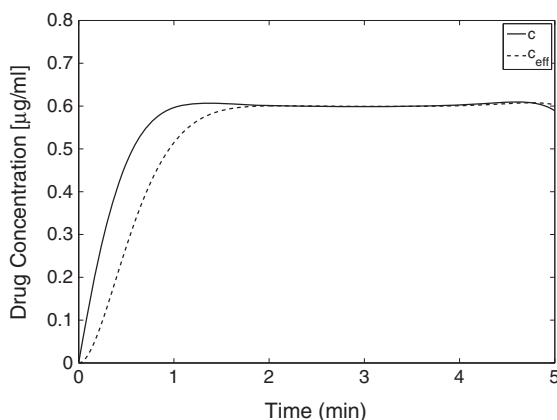


Figure 3. Drug concentration $c(t) = \frac{x_1(t)}{V_c}$ and $c_{\text{eff}}(t)$ as a function of time.

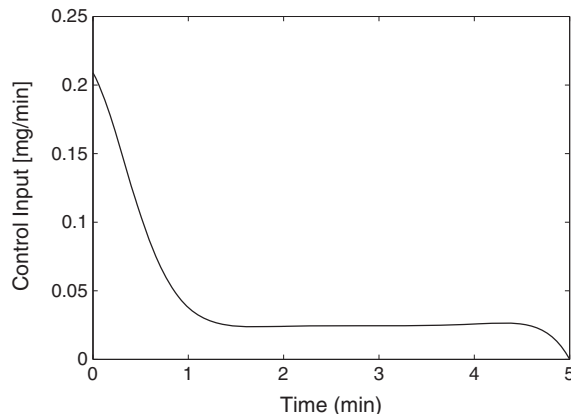


Figure 4. Control input as a function of time.

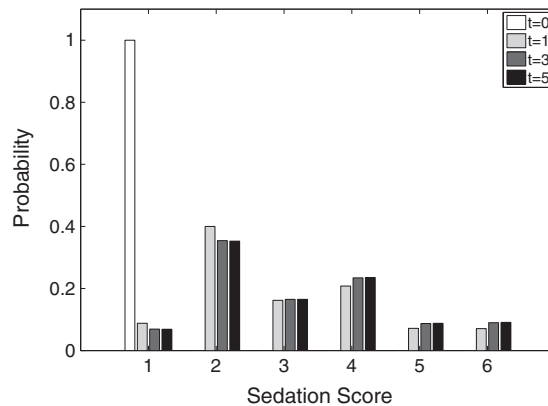


Figure 5. Probability mass function for sedation score $S(t)$ for $t = 0, 1, 3,$ and 5 .

8. DISCUSSION AND DIRECTIONS FOR FUTURE RESEARCH

The distribution of sedation scores given in Figure 5 reflects equation (37) and the effect of drug concentrations that result from the infusion illustrated in Figure 4. At $t = 5$ min, the drug concentration at the effect-side compartment c_{eff} reaches the target level given by (15). The reader will note that the mode of the distribution at $t = 5$ min is actually a score of 2 rather than the target of 3. However, this distribution is in fact the closest achievable sedation score distribution in the family of distributions defined by (37) to the ‘ideal’ distribution given by (9) using the weighted norm $\|\cdot\|_Q$. In addition, the penalty implicit in the term $r_2 u^2$ in (20) included in $L(x(t), u(t))$ penalizes rapid infusion of the drug and is a reflection of how clinicians actually administer propofol. The clinician has no a priori knowledge of how the patient will respond to propofol, and although achievement of adequate sedation is important, it cannot be achieved at the cost of an overdose with subsequent cardiovascular compromise. Thus, the typical behavior of clinicians is to administer the drug relatively slowly.

It should be emphasized that this optimal control strategy is not adaptive and is inherently challenged by interpatient variability. Implementation will require clinical investigation to find the ‘best’ parameters, including those reflective of interpatient variability (pharmacokinetic and pharmacodynamic parameters) as well as those that quantify the deviation of the sedation score distribution from the ideal distribution, and penalize overdoses (i.e., Q , R_1 , r_2 , and c_{max}). And although this is a shortcoming of any optimal control strategy, this approach is inherently conservative and errs on the side of safety (as demonstrated by the mode of the distribution of sedation scores shown in Figure 5) because it does have these penalty terms. Actual clinical implementation would have to allow the clinician to ‘tune’ the parameters in real time (as in the OR or ICU), and given the multiplicity of these parameters, it might be best to have the option to tune R_1 and r_2 because they penalize deviation from the ideal sedation score distribution as well as overdoses, and this is the thing the clinician most wants to prevent. We have not yet investigated the simple option of changing either R_1 or r_2 in real time.

Finally, note that the drug infusion illustrated in Figure 4 resembles the input that skilled clinicians usually create when administering propofol manually. It begins with a rapid infusion rate that rapidly declines to a plateau value. Multiple investigations in the anesthesia literature confirm that a target blood concentration of propofol (and almost all other drugs) is best achieved by this type of algorithm, whether administered continuously as loading dose followed by exponentially declining infusions [21], or by an approximation with an instantaneous loading dose followed by stepwise decreasing infusions [22]. The authors in [6] have investigated ICU sedation by using a pharmacokinetic–pharmacodynamic model, but it is neither an adaptive nor an optimal control strategy. Several investigators have developed adaptive closed-loop control models for operative anesthesia by using processed EEG feedback (e.g., [23]), but the goals of operative anesthesia are

quite distinct from ICU sedation. To our knowledge, this is the first investigation of optimal control for ICU sedation. Thus, it is very difficult to compare our results with other standard methods, other than to note that the infusion scheme is quite similar to what an expert clinician would create using manual administration.

9. CONCLUSION

In this paper, we modeled the pharmacokinetics and pharmacodynamics of a general sedative agent by using a hybrid deterministic–stochastic model involving deterministic pharmacokinetics and stochastic pharmacodynamics. Specifically, we used nonnegative and compartmental modeling to model the pharmacokinetics of propofol, and a stochastic process to represent the patient's sedation score and model the pharmacodynamics of propofol. Next, we used this deterministic–stochastic model to develop an open-loop optimal control policy for ICU sedation. Specifically, we first found the optimal effect-site drug concentration corresponding to a high probability for the desired sedation score (i.e., MRSS score of 3) and a low probability for all other sedation scores. Then, we used optimal control theory to drive the effect-site drug concentration to the optimal value found in the previous step while minimizing a given cost functional.

ACKNOWLEDGEMENT

The first-named author acknowledges several fruitful discussions with Professor Prasad Tetali.

REFERENCES

1. Devlin J, Boleski G, Mlynarek M, Nerenz D, Peterson E, Jankowski M, Horst H, Zarowitz B. Motor activity assessment scale: a valid and reliable sedation scale for use with mechanically ventilated patients in an adult surgical intensive care unit. *Critical Care Medicine* 1999; **1**:1271–1275.
2. Sessler C, Gosnell M, Grap MJ, Brophy G, O'Neal P, Keane K, Tesoro E, Elswick R. The Richmond agitation–sedation scale. *American Journal of Respiratory and Critical Care Medicine* 2002; **166**:1338–1344.
3. Ramsay MAE, Savege TM. Controlled sedation with alphaxalone–alphadolone. *British Medical Journal* 1974; **2**:656–659.
4. Haddad WM, Chellaboina V, Hui Q. *Nonnegative and Compartmental Dynamical Systems*. Princeton University Press: Princeton, NJ, 2010.
5. Haddad WM, Bailey JM. Closed-loop control for intensive care unit sedation. *Best Practice & Research Clinical Anaesthesiology* 2009; **23**:95–114.
6. Barr J, Egan TD, Sandoval NF, Zomorodi K, Cohane C, Gambus PL, Shafer SL. Propofol dosing regimens for ICU sedation based upon an integrated pharmacokinetic–pharmacodynamic model. *Anesthesiology* 2001; **95**:324–333.
7. Barr J, Zomorodi K, Bertaccini EJ, Shafer SL, Geller E. A double-blind, randomized comparison of IV lorazepam versus midazolam for sedation of ICU patients via a pharmacologic model. *Anesthesiology* 2001; **95**:286–298.
8. Boyd S, Vandenberghe L. *Convex Optimization*. Cambridge University Press: Cambridge, UK, 2004.
9. Gilman AG, Hardman JG, Limbird LE. *Goodman and Gilman's the Pharmacological Basis of Therapeutics*, 10th edn. McGraw-Hill: New York, NY, 1996.
10. Kazama T, Ikeda K, Morita K. The pharmacodynamic interaction between propofol and fentanyl with respect to the suppression of somatic or hemodynamic responses to skin incision, peritoneum incision, and abdominal wall retraction. *Anesthesiology* 1998; **89**(4):894–906.
11. Schnider TW, Minto CF, Stanski DR. The effect compartment concept in pharmacodynamic modelling. *Anaesthetic Pharmacology Review* 1994; **2**:204–219.
12. Bryson AE, Ho YC. *Applied Optimal Control*. Ginn and Company: Waltham, MA, 1969.
13. Marsh B, White M, Morton N, Kenny GN. Pharmacokinetic model driven infusion of propofol in children. *British Journal of Clinical Anaesthesia* 1991; **67**(1):41–48.
14. Upton RN, Ludbrook GI, Grant C, Martinez A. Cardiac output is a determinant of the initial concentration of propofol after short-term administration. *Anesthesia and Analgesia* 1999; **89**(3):545–552.
15. Muzi M, Berens RA, Kampine JP, Ebert TJ. Venodilation contributes to propofol-mediated hypotension in humans. *Anesthesia and Analgesia* 1992; **74**(6):877–883.
16. Ismail EF, Kim SJ, Salem MR. Direct effects of propofol on myocardial contractility in situ canine hearts. *Anesthesiology* 1992; **79**(5):964–972.
17. Hill AV. The possible effects of the aggregation of the molecules of haemoglobin on its dissociation curves. *Journal of Physiology* 1910; **40**(1):iv–vii.
18. Hayakawa T, Haddad WM, Bailey JM, Hovakimyan N. Passivity-based neural network adaptive output feedback control for nonlinear nonnegative dynamical systems. *IEEE Transactions Neural Networks* 2005:387–398.

19. Kazama T, Ikeda K, Morita K, Kikura M, Doi M, Ikeda T, Kurita T. Comparison of the effect site KeOs of propofol for blood pressure and EEG bispectral index in elderly and young patients. *Anesthesiology* 1999; **90**:1517–1527.
20. Eckenhoff RG, Johansson JS. On the relevance of “clinically relevant concentrations” of inhaled anesthetics in in vitro experiments. *Anesthesiology* 1999; **91**(3):856–860.
21. Bailey JM, Shafer SL. A simple analytical solution to the three compartment pharmacokinetic model suitable for computer controlled infusion pumps. *IEEE Transactions on Biomedical Engineering* 1991; **38**:522–525.
22. Bailey JM. A technique for approximately maintaining constant plasma levels of intravenous drugs. *Anesthesiology* 1993; **78**:116–123.
23. Struys M, De Smet T, Versichelen L, Van de Vilde S, Van den Broecke R, Mortier E. Comparison of closed-loop controlled administration of propofol using BIS as the controlled variable versus ‘standard practice’ controlled administration. *Anesthesiology* 2001; **95**(1):6–17.